



## Ni modified ceramic anodes for solid oxide fuel cells

Guoliang Xiao<sup>a</sup>, Chao Jin<sup>a,b</sup>, Qiang Liu<sup>a</sup>, Andreas Heyden<sup>c</sup>, Fanglin Chen<sup>a,\*</sup>

<sup>a</sup> Department of Mechanical Engineering, University of South Carolina, Columbia, SC 29208, USA

<sup>b</sup> School of Physical Science and Technology, College of Energy, Soochow University, Suzhou 215006, PR China

<sup>c</sup> Department of Chemical Engineering, University of South Carolina, Columbia, SC 29208, USA

### ARTICLE INFO

#### Article history:

Received 23 August 2011

Received in revised form 26 October 2011

Accepted 30 October 2011

Available online 4 November 2011

#### Keywords:

Solid oxide fuel cells

Perovskite oxides

Ni

Impregnation

### ABSTRACT

Ni modified  $\text{Sr}_2\text{Fe}_{1.5}\text{Mo}_{0.5}\text{O}_6$  (SFM) and  $\text{La}_{0.75}\text{Sr}_{0.25}\text{Cr}_{0.5}\text{Mn}_{0.5}\text{O}_3$  (LSCM) anodes have been studied as anode materials for solid oxide fuel cells (SOFCs). Temperature-programmed reduction (TPR) results show that Ni promotes the oxidation of  $\text{H}_2$  on SFM. As a result, a cell with Ni-SFM as the anode,  $\text{La}_{0.8}\text{Sr}_{0.2}\text{Ga}_{0.83}\text{Mg}_{0.17}\text{O}_3$  (LSGM) as the electrolyte, and  $\text{La}_{0.6}\text{Sr}_{0.4}\text{Co}_{0.2}\text{Fe}_{0.8}\text{O}_3$  (LSCF) as the cathode shows a high peak power density of  $1166 \text{ mW cm}^{-2}$  at  $800^\circ\text{C}$  using  $\text{H}_2$  as the fuel and ambient air as the oxidant. Ni modified SFM also shows enhanced performance in  $\text{CH}_4$  (with 3 vol%  $\text{H}_2\text{O}$ ). Compared with SFM, Ni-SFM anode demonstrates enhanced catalytic activity, resulting in higher open-circuit voltage and lower electrode polarization resistance in  $\text{CH}_4$ . However, due to the presence of Ni, the sulfur tolerance of these Ni-modified anodes is still low. The cell performance drops by almost 18% after the cell with Ni-SFM anode has been operating for 20 h in a fuel of  $\text{H}_2$  with 100 ppm  $\text{H}_2\text{S}$  at  $800^\circ\text{C}$ . However, the cell performance can be fully recoverable upon removal of  $\text{H}_2\text{S}$  from the fuel stream. Similar cell performance improvements have also been observed on cells with Ni modified LSCM anodes. The cells with the Ni-LSCM anodes have shown relatively stable performance during the short-term durability test at  $800^\circ\text{C}$  in  $\text{CH}_4$  at  $800^\circ\text{C}$ .

© 2011 Elsevier B.V. All rights reserved.

### 1. Introduction

The intrinsic high efficiency in energy conversion of solid oxide fuel cells (SOFCs) makes them promising devices for generating electricity. In order to improve their performance in various fuels, alternative anode materials have recently received a lot of attentions [1–5]. Compared with the conventional Ni-based cermet anode, ceramic materials show advantages in their stabilities when the cell is fed with fuels containing hydrocarbons and hydrogen sulfide or cycled in different atmospheres [6]. However, their overall cell performance is still relatively low and needs to be improved. Generally, the performance of ceramic anode materials is limited by their electrical conductivity and catalytic activity. In some cases, the cell performance can be improved dramatically by introducing a small amount of precious metal catalysts. This indicates that the catalytic activity of the ceramic materials may be a restraint on improving their performance [7,8].

Among the non-precious metal catalysts, Ni is an important one that shows high catalytic activity for  $\text{H}_2$  oxidation and many other hydrocarbon reforming reactions but suffers from coke deposition [9,10]. However, such degradation issues of Ni catalysts can be suppressed by dispersion of the Ni catalyst on

appropriate catalyst supports [11]. Most ceramic anode materials are mixed ionic and electronic conductors (MIECs), a property that may promote catalytic oxidation reactions, making them potential supports for Ni with coke suppression capability. Recently, Ni has been applied to ceramic anodes as a catalyst [12]. By impregnating  $\text{La}_{0.75}\text{Sr}_{0.25}\text{Cr}_{0.5}\text{Mn}_{0.5}\text{O}_3$  (LSCM) with some Ni, the fuel cell performance in both hydrogen and methane has been enhanced dramatically. At  $850^\circ\text{C}$ , the peak power density was  $362 \text{ mW cm}^{-2}$  in  $\text{CH}_4$  for YSZ electrolyte-supported single cells using Ni-modified LSCM as anodes, which is much higher than the power density of cells with pure LSCM anode [13]. Similar improvements on the cell performance have also been observed on  $\text{Sr}_2\text{Fe}_{1.5}\text{Mo}_{0.5}\text{O}_6$  (SFM) by our group [14]. Benefited from the redox-stable ceramic material, the cells with the anodes modified by Ni also showed good redox stability [15]. Overall, these results suggest that Ni-modification may be considered as a promising strategy to modify ceramic anodes.

In this work, the catalytic activity and cell performance of Ni modified SFM and LSCM anodes have been studied.

### 2. Experimental

#### 2.1. Material preparation

SFM and LSCM were made by a combustion method. The metal precursors were  $\text{Sr}(\text{NO}_3)_2$ ,  $\text{Fe}(\text{NO}_3)_3 \cdot 9\text{H}_2\text{O}$ ,  $(\text{NH}_4)_6\text{Mo}_7\text{O}_{24} \cdot 4\text{H}_2\text{O}$ ,

\* Corresponding author. Tel.: +1 803 777 4875; fax: +1 803 777 0106.  
E-mail address: [chenfa@cec.sc.edu](mailto:chenfa@cec.sc.edu) (F. Chen).

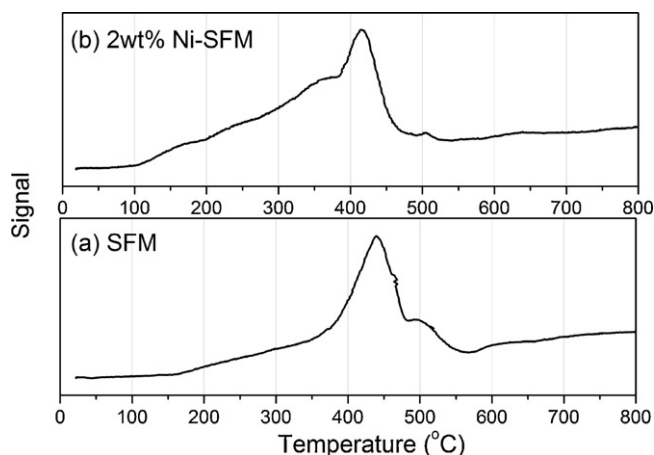


**Fig. 1.** Influence of Ni on the reduction profiles of (a) SFM and (b) Ni-SFM. The curves were recorded in 5% H<sub>2</sub> in Ar at a ramp rate of 10 °C min<sup>-1</sup>. The powders were degassed and reoxidized at 400 °C before testing.

La(NO<sub>3</sub>)<sub>3</sub>·6H<sub>2</sub>O, Cr(NO<sub>3</sub>)<sub>3</sub>·9H<sub>2</sub>O and Mn(NO<sub>3</sub>)<sub>2</sub>·4H<sub>2</sub>O which were all purchased from Alfa Aesar. For synthesis of SFM, citric acid was used to adjust the pH value of the ammonium molybdate solution to prevent precipitation of other metal cations. Glycine was used as the combustion agent for both SFM and LSCM. After the combustion process, the precursor powders of SFM and LSCM were fired at 1000 °C and 1100 °C respectively for 5 h to form the pure phase. La<sub>0.6</sub>Sr<sub>0.4</sub>Co<sub>0.2</sub>Fe<sub>0.8</sub>O<sub>3</sub> (LSCF) was also synthesized by a similar combustion method. Citric acid was used as the fuel. The LSCF powder was obtained by firing the precursor at 1050 °C for 5 h. La<sub>0.8</sub>Sr<sub>0.2</sub>Ga<sub>0.83</sub>Mg<sub>0.17</sub>O<sub>3</sub> (LSGM) electrolyte powders were made by the solid-state reaction method described elsewhere [16].

Crystalline structures and phases of all the powders were evaluated by powder X-ray diffraction (XRD). The XRD experiment was conducted on a D/MAX-3C X-ray diffractometer equipped with a graphite monochromator. Cu K<sub>α</sub> radiation ( $\lambda = 1.5418 \text{ \AA}$ ) was used. The scanning rate was 5 ° min<sup>-1</sup>. Microstructures of the Ni modified ceramic materials were studied by a scanning electron microscope (SEM, FEI Quanta and XL 30) equipped with a secondary electron detector. The accelerating voltage was 30 kV. The Ni loading amount was determined by an energy dispersive X-ray spectrometer (EDX) of the SEM on the anode area.

## 2.2. Temperature-programmed reduction (TPR)

For the TPR experiment, the Ni modified samples were prepared by grinding a mixture of SFM and Ni(NO<sub>3</sub>)<sub>2</sub>·6H<sub>2</sub>O in an ethanol medium. The mixture was dried and annealed at 500 °C in air for 1 h. The Ni loading amount was set as 2 wt% according to the value in the impregnated anode in cell tests.

Before the TPR test, the powder was degassed at 400 °C in N<sub>2</sub> followed by a re-oxidation in 10% O<sub>2</sub> at the same temperature. The sample was subsequently cooled down to room temperature and the TPR data was collected in 5% H<sub>2</sub> in Ar with a ramp rate of 10 °C min<sup>-1</sup> from room temperature to 800 °C.

## 2.3. Cell testing

Electrolyte-supported cells were prepared for cell testing. LSGM electrolyte pellets were sintered at 1400 °C for 5 h and their thickness was about 250 μm. Electrode inks were made by mixing the electrode powders with a commercial binder (Heraeus V006) in a weight ratio of 1:1.5.

For the cells with SFM anode, the anode and cathode were printed on each side of LSGM electrolyte pellets and co-fired in

air at 1100 °C for 1 h. The cells with LSCM anode were prepared in two steps. The LSCM|LSGM half cells were fired in air at 1250 °C for 2 h. Subsequently, the LSCF cathode was painted on the other side of the LSGM electrolyte and fired in air at 1100 °C for 1 h. The effective cathode area was about 0.33 cm<sup>2</sup>.

To make Ni-modified anodes, a 0.5 M Ni(NO<sub>3</sub>)<sub>2</sub> solution was used to impregnate the ceramic anode. The cell was then fired at 500 °C for 1 h prior to the cell testing. According to the EDX analysis, the Ni loading amount on the ceramic anodes was about 2 wt%.

Au paste was screen-printed on the anode surface to form a current collection layer on the anode. Each electrode was connected with two lead wires for current and voltage measurements. Electrochemical characterization of the cells was conducted with a Versa STAT 3-400 test system (Princeton Applied Research). Ambient air was used as the oxidant. The flow rate of the fuel gas was set at 40 ml min<sup>-1</sup>.

## 3. Results and discussion

### 3.1. TPR study

Ni plays an important catalytic role in the Ni-based cermets anode for oxidation of H<sub>2</sub>. In order to investigate the improvement on the catalytic activity of Ni modified MIECs, TPR was carried out on SFM and Ni-modified SFM samples. As shown in Fig. 1a, there are mainly two reduction peaks for pure SFM. One starts around 170 °C and reaches the maximum at about 440 °C. The other shoulder peak is located around 500 °C. Considering that there are two multi-valence cations, Fe and Mo in the SFM composition, these two reduction peaks may be related to their reductions to lower valence states. As shown in Fig. 1b, the TPR profiles of Ni-modified SFM are quite different from those of the pure SFM. The intensity of the shoulder peak around 500 °C decreases and an additional peak appears around 360 °C. The reduction signal also starts at a lower temperature around 110 °C. Even for the strongest reduction peak, the location of its maximum shifts to around 420 °C. Such TPR features are indicative of the interaction between Ni and the SFM during the reduction process, which in turn makes the oxidation of hydrogen on Ni-modified SFM easier. In other words, the catalytic activity of Ni-modified SFM for hydrogen oxidation seems to be significantly improved by the addition of Ni in the SFM anode.

### 3.2. Cell performance in hydrogen

The catalytic activity of SFM with or without Ni modification was studied in a single cell test. Fig. 2 shows the SEM images of the SFM anode before and after infiltration with Ni. Since the Ni loading amount is relatively small and the pre-treatment temperature is only 500 °C, there is no significant difference in the SFM microstructure. Additionally, from the enlarged images (Fig. 2b and d), the Ni particles can still not be distinguishable, suggesting that Ni has been well dispersed on the surface of SFM particles. The performance of the cell with the configuration of Ni-SFM|LSGM|LSCF is shown in Fig. 3 (solid dots) with H<sub>2</sub> (3 vol% H<sub>2</sub>O) as the fuel and ambient air as the oxidant. The peak power density of the cell reaches 559, 828, and 1166 mW cm<sup>-2</sup> at 700, 750, and 800 °C, respectively, demonstrating the cell performance of the Ni modified SFM anode is significantly higher than that of the cells with the SFM anode (open dots) tested under similar conditions. The performance of the cells with Ni-modified anodes is also higher than that of cells containing other pure ceramic anode materials [17,18]. The improvement in cell performance suggests that Ni has significantly improved the catalytic activity of the Ni-SFM anode in H<sub>2</sub>.

Fig. 4 shows the impedance spectra of the cells with the configuration of Ni-SFM|LSGM|LSCF (solid dots) and SFM|LSGM|LSCF

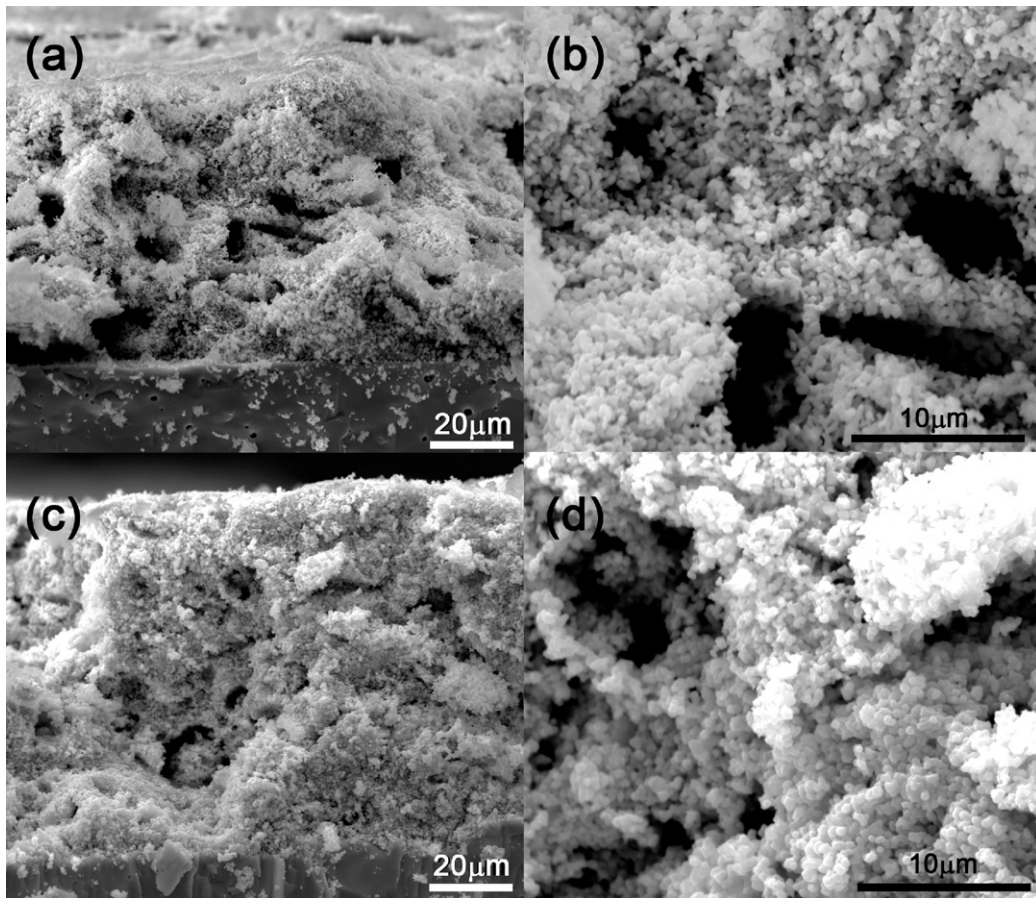


Fig. 2. SEM images of SFM anode (a and b) and Ni-SFM (c and d).

(open dots) using  $H_2$  as the fuel under open-circuit conditions at different temperatures. Each spectrum consists of several arcs. The high frequency intercept of the impedance spectra with the real axis represents the cell ohmic resistance ( $R_{ohm}$ ), which includes the resistances from the electrolyte, electrodes and the contact between them. The low frequency intercept represents the total resistance of the cell ( $R_{total}$ ). The difference between them represents the cell polarization resistance ( $R_p$ ) attributed to the electrode

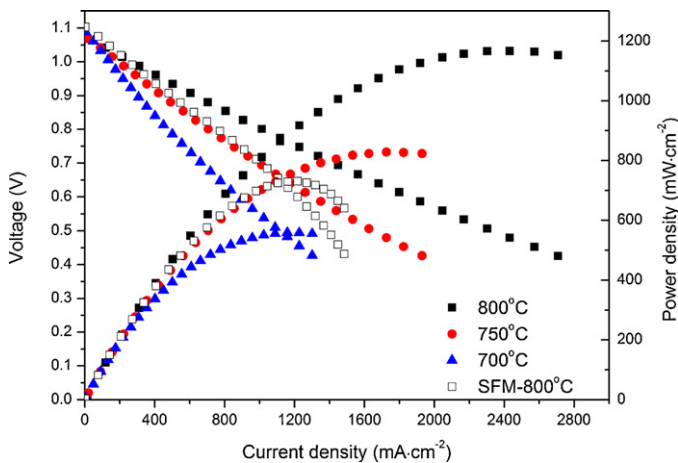


Fig. 3. Cell voltage and power density versus current density in wet  $H_2$  (3 vol%  $H_2O$ ) of the single cell Ni-SFM|LSGM|LSCF at different temperatures (solid dots) and SFM|LSGM|LSCF at 800 °C (open dots).

reactions. It is noticeable that  $R_{ohm}$  for the cell with the Ni-SFM anode is different from that of the cell with the SFM anode at 800 °C. It is probably due to the slight difference in the thickness of the electrolyte membranes used for the cells. The cell polarization resistance is only about  $0.145 \Omega \text{ cm}^2$  for the cell with the Ni-SFM anode at 800 °C which is much lower than that of the cell with pure SFM, about  $0.243 \Omega \text{ cm}^2$ , under the same testing conditions, indicating good catalytic activity of the Ni-SFM anode. It can be observed that the high frequency arc of the cell impedance spectra of the cells with the Ni-SFM anodes decreases with the increase of the cell operating temperature from 700 to 800 °C. The temperature dependences of  $R_{ohm}$ ,  $R_p$  and  $R_{total}$  for the cell with the Ni-SFM anode are shown in Fig. 5. It can be seen that  $R_p$  is more dominant in  $R_{total}$  than  $R_{ohm}$  at lower temperatures. However,  $R_{ohm}$  becomes more dominant when the temperature is above 800 °C. The ratio of  $R_p$  to  $R_{total}$  decreases from 57% at 700 °C to 49% at 800 °C.  $R_{ohm}$  comes primarily from the LSGM membrane based on the thickness of the LSGM electrolyte and the conductivity of LSGM [16]. Therefore, it can be expected

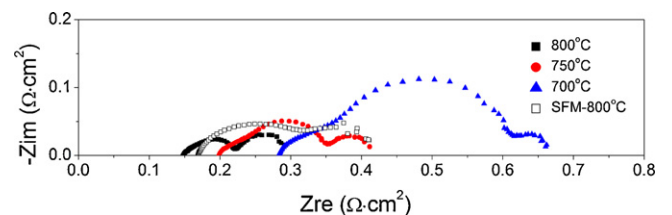


Fig. 4. Impedance spectra of the cell Ni-SFM|LSGM|LSCF at different temperatures (solid dots) and SFM|LSGM|LSCF at 800 °C (open dots).

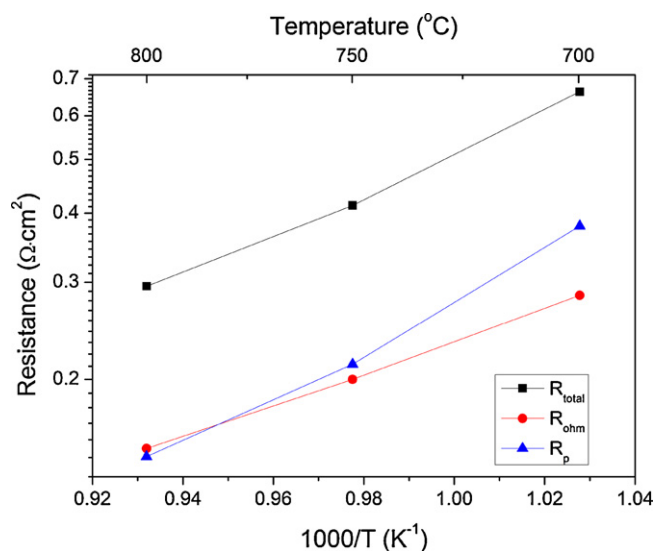


Fig. 5. Resistances of the cell Ni-SFM|LSGM|LSCF at 700, 750 and 800 °C in H<sub>2</sub> under open-circuit conduction.

that the cell performance can be further improved if the thickness of electrolyte is reduced.

### 3.3. Cell performance in methane

Compared with H<sub>2</sub>, it is more challenging for ceramic anode materials to use hydrocarbon fuels due to their low catalytic activity. The effect of Ni was investigated by characterizing the electrochemical performance of the single cells in CH<sub>4</sub> (with 3 vol% H<sub>2</sub>O) with the Ni-SFM anode. The open-circuit voltage (OCV) of the cells was monitored when the fuel was switched from H<sub>2</sub> to CH<sub>4</sub>. Fig. 6 shows that the OCVs of the cells with Ni-SFM and SFM anodes both initially dropped. After about 10 h, the OCV of each cell became stable, suggesting that there is no serious coking problem in the anode or degradation of the cell under open circuit conditions. At 800 °C in CH<sub>4</sub> (with 3 vol% H<sub>2</sub>O), the OCV of the cell with the pure SFM anode is only about 0.77 V while that of the one with the Ni-SFM anode reaches 0.98 V. Generally, the theoretical

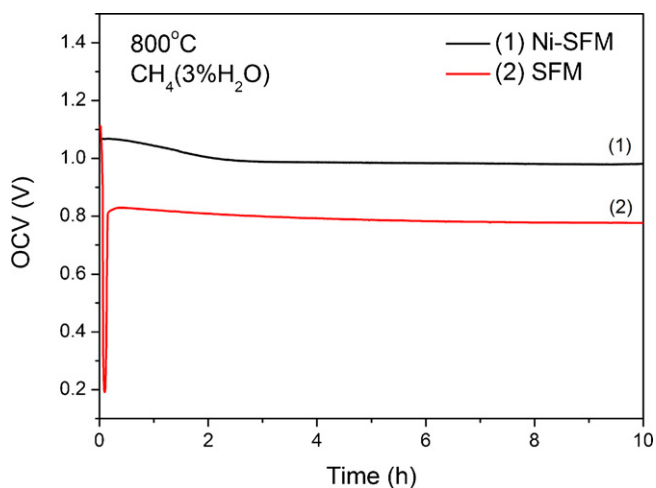


Fig. 6. Open-circuit voltage of the cells with the (1) Ni-SFM anode and (2) SFM anode in wet CH<sub>4</sub> (3 vol% H<sub>2</sub>O) at 800 °C.

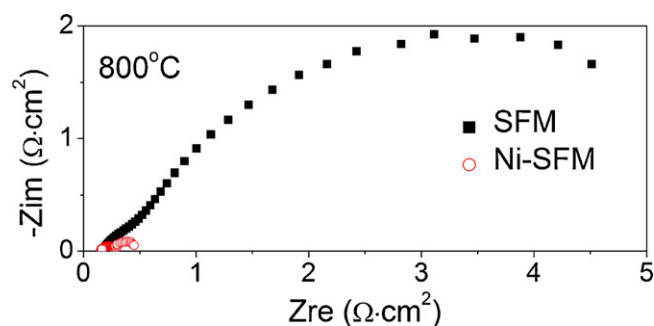


Fig. 7. Impedance spectra of single cells with the Ni-SFM anode and SFM anode in wet CH<sub>4</sub> (3 vol% H<sub>2</sub>O) at 800 °C under open-circuit conditions.

reversible potential  $E$  of the SOFCs with oxide ionic conductors as the electrolyte can be determined by the Nernst equation [19]:

$$E = \frac{RT}{4F} \ln \frac{P_{O_2}^a}{P_{O_2}^c} \quad (1)$$

where  $R$ ,  $T$ ,  $F$ ,  $P_{O_2}^a$  and  $P_{O_2}^c$  denote the universal gas constant, the cell operating temperature, the Faraday's constant and the oxygen partial pressures in the anode and cathode, respectively. For SOFCs using hydrocarbon fuels, due to the different catalytic activity of the anode materials, the fuel reaction mechanism may vary, consequently resulting in a different composition of gas species in the anode which determines the specific  $P_{O_2}^a$  on the anode surface and in turn changes the potential of the cell. In other words, the OCV of the cell in methane can reflect the catalytic activity of the anode material for methane oxidation. Therefore, the improved OCV shown in Fig. 6 suggests that the catalytic activity of the SFM anode in methane is improved by loading very small amount of Ni in SFM.

The improved catalytic activity in methane of the Ni-SFM anode can be further seen from the cell impedance spectra. As shown in Fig. 7, the cell with the SFM anode shows very large cell polarization resistance in methane, which is more than 4.5 Ω cm<sup>2</sup>. However, the polarization resistance of the cell with Ni-SFM anode drops to 0.3 Ω cm<sup>2</sup>. Such a change in the cell polarization results in a great improvement of the cell performance in methane for the cell with the Ni-SFM anode. As we have previously reported, the peak power density reaches up to 600 mW cm<sup>-2</sup> in CH<sub>4</sub> (with 3 vol% H<sub>2</sub>O) at 800 °C for the cells with the Ni-SFM anodes, which is more than ten times higher than that of the cells with pure SFM anodes [14].

### 3.4. Sulfur tolerance

Although the fuel oxidation on ceramic materials can be significantly promoted by dispersion of a small amount of Ni, Ni can also be poisoned by trace levels of H<sub>2</sub>S in the fuel. Consequently, the sulfur tolerance of the Ni modified SFM anode needs to be investigated. Fig. 8a shows the current density of the cell Ni-SFM|LSGM|LSCF operated at a constant voltage of 0.7 V at 800 °C after the fuel gas being switched from H<sub>2</sub> to H<sub>2</sub> with 100 ppm H<sub>2</sub>S. A continuous cell performance drop can be seen when the cell is operated in H<sub>2</sub> with 100 ppm H<sub>2</sub>S. After about 20 h, the cell current density drops from 1.34 to 1.1 A cm<sup>-2</sup>. Such a degradation rate in H<sub>2</sub> with 100 ppm H<sub>2</sub>S is much higher than that observed on a SFM anode with a similar composition in our previous study [18], suggesting that the cell degradation is mainly due to the presence of Ni in the Ni-SFM anode. It can be seen from Fig. 8b that the cell polarization resistance has increased from 0.15 to almost 0.19 Ω cm<sup>2</sup> after the cell has been operated at a constant voltage load of 0.7 V in H<sub>2</sub> with 100 ppm H<sub>2</sub>S. On the other hand it also indicates that the electrode activity is significantly affected by the Ni loaded on SFM. However,

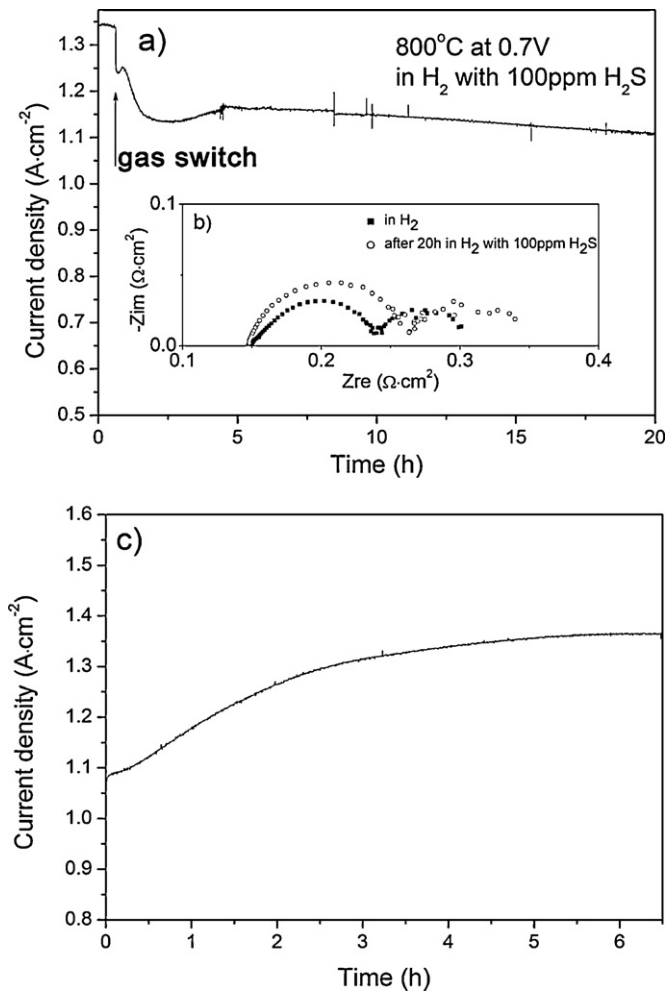


**Fig. 8.** (a) Performance of the cell Ni-SFM|LSGM|LSCF in  $\text{H}_2$  with 100 ppm  $\text{H}_2\text{S}$  at 0.7 V at  $800^\circ\text{C}$ , (b) impedance spectra of the cell in  $\text{H}_2$  and after stability test in 100 ppm  $\text{H}_2\text{S}$  at  $800^\circ\text{C}$ , and (c) performance of the cell in  $\text{H}_2$  at 0.7 V at  $800^\circ\text{C}$  after exposing to 100 ppm  $\text{H}_2\text{S}$ .

benefited from the large content of SFM in the anode, the cell performance can be fully recovered upon removing  $\text{H}_2\text{S}$  from the fuel gas, as shown in Fig. 8c.

### 3.5. Cell performance with different ceramic components

The cell performance of the LSCM anode modified by a similar amount of Ni ( $\sim 2$  wt%) in a similar cell configuration (i.e., Ni-LSCM|LSGM|LSCF) has also been studied. As demonstrated in Fig. 9a, at  $800^\circ\text{C}$ , the cell peak power density is about  $802 \text{ mW cm}^{-2}$  in  $\text{H}_2$  (with 3 vol%  $\text{H}_2\text{O}$ ) and  $425 \text{ mW cm}^{-2}$  in  $\text{CH}_4$  (with 3 vol%  $\text{H}_2\text{O}$ ). The cell performance of the cells with the Ni-LSCM anodes is slightly lower than that of the cells with the Ni-SFM anodes, probably due to the different properties of the ceramic component in the anode. The impedance spectra of the cell in different fuels under open-circuit condition are shown in Fig. 9b. The cell polarization resistance is about  $0.19 \Omega \text{ cm}^2$  in  $\text{H}_2$  and  $0.52 \Omega \text{ cm}^2$  in  $\text{CH}_4$  at  $800^\circ\text{C}$ , comparable to that of the cells with the Ni-SFM anodes.

The OCV and polarization resistance in  $\text{CH}_4$  of the Ni modified SFM and LSCM obtained in this work as well as those reported in the literature are summarized in Table 1. With different ceramic components, the increased OCV and reduced cell polarization resistance are observed for ceramic anodes with inclusion of Ni, suggesting that Ni modified ceramic anodes show more attractive

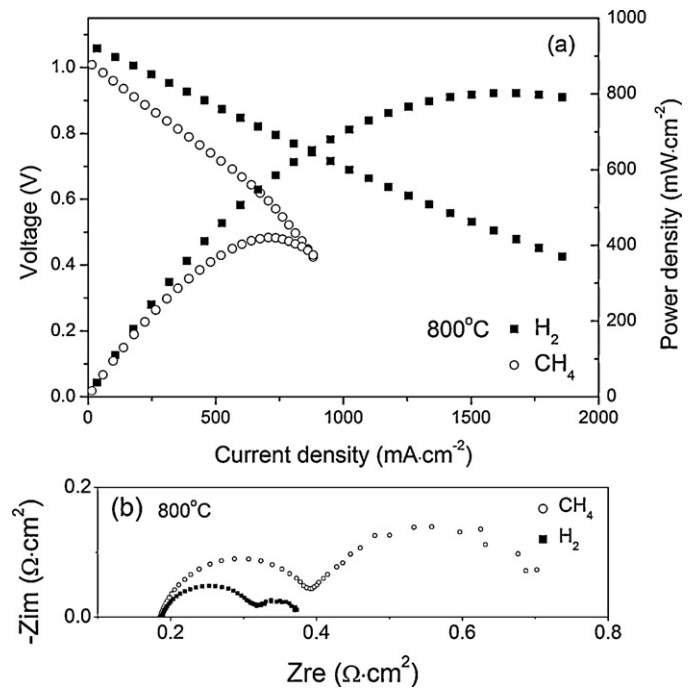


**Fig. 9.** (a) Cell voltage and power density versus current density in wet  $\text{H}_2$  (3 vol%  $\text{H}_2\text{O}$ ) and wet  $\text{CH}_4$  (3 vol%  $\text{H}_2\text{O}$ ) of the single cell Ni-LSCM|LSGM|LSCF at  $800^\circ\text{C}$  and (b) impedance spectrum of the cell at  $800^\circ\text{C}$  under open-circuit conditions.

performance in  $\text{CH}_4$  than the anode of the pure ceramic materials [13,14,17,18,20].

The stability of the Ni-LSCM anode in  $\text{CH}_4$  was investigated by operating the cell at 0.7 V at  $800^\circ\text{C}$ . The current density of the cell was recorded and is shown in Fig. 10. An activation process can be observed in the first 7 h that the current density has increased from 510 to  $610 \text{ mA cm}^{-2}$ . When the cell is operated under a certain current, oxygen ions will be continuously transferred to the anode side. This may further improve the anode catalytic activity for methane reforming and in turn improve the cell performance. The cell performance is relatively stable in the short-term stability test.

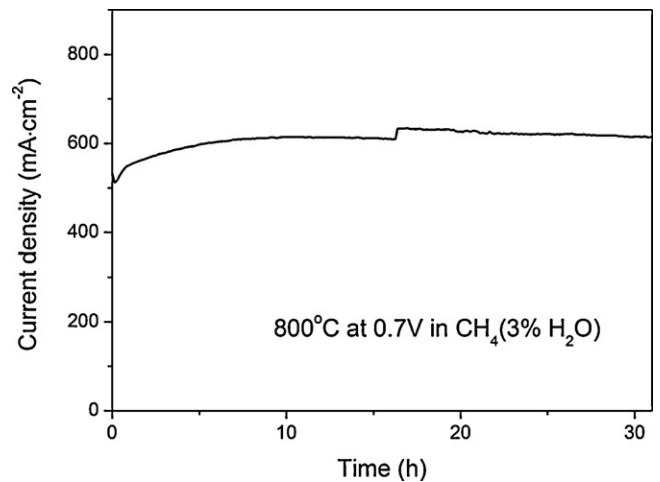


**Fig. 10.** Performance of the cell Ni-LSCM|LSGM|LSCF in  $\text{CH}_4$  (3 vol%  $\text{H}_2\text{O}$ ) at 0.7 V at  $800^\circ\text{C}$ .

**Table 1**  
Open-circuit voltage (OCV) and polarization resistance of single cells with different anode materials in methane.

Anode materials	Test conditions	OCV (V)	Polarization resistance ( $\Omega \text{ cm}^2$ )
SFM	CH <sub>4</sub> (3 vol% H <sub>2</sub> O), 800 °C	0.77	4.5
~2 wt% Ni-SFM	CH <sub>4</sub> (3 vol% H <sub>2</sub> O), 800 °C	0.98	0.3
~2 wt% Ni-LSCM	CH <sub>4</sub> (3 vol% H <sub>2</sub> O), 800 °C	1.02	0.52
LSCM [13]	Dry CH <sub>4</sub> , 850 °C	0.8	–
~11 wt% Ni-LSCM [13]	Dry CH <sub>4</sub> , 850 °C	0.94	–

#### 4. Conclusions

A small amount of Ni (~2 wt%) has been dispersed on SFM and LSCM to improve their catalytic activity. The TPR and single cell test results show that the catalytic activity of these ceramic materials in both hydrogen and methane has been significantly improved. Due to the sulfur poisoning of Ni, the cell with the Ni-SFM anode has showed performance degradation when operating in H<sub>2</sub> with 100 ppm H<sub>2</sub>S as the fuel, but such degradation can be recovered upon removing H<sub>2</sub>S from the fuel stream. Cells with the Ni modified ceramic anodes have demonstrated relatively good stability in short term operations when using CH<sub>4</sub> as the fuel.

#### Acknowledgements

This work has been financially supported by the HeteroFoam Center (Heterogeneous Functional Materials for Energy Systems), an Energy Frontier Research Center funded by the DoE Office of Basic Energy Sciences under Award Number DE-SC0001061.

#### References

[1] R.M. Ormerod, Chem. Soc. Rev. 32 (2003) 17–28.

- [2] A. Atkinson, S. Barnett, R.J. Gorte, J.T.S. Irvine, A.J. McEvoy, M.B. Mogensen, S. Singhal, J. Vohs, Nat. Mater. 3 (2004) 17–27.
- [3] Z.L. Zhan, S.A. Barnett, Science 308 (2005) 844–847.
- [4] M.D. Gross, J.M. Vohs, R.J. Gorte, J. Mater. Chem. 17 (2007) 3071–3077.
- [5] D.J.L. Brett, A. Atkinson, N.P. Brandon, S.J. Skinner, Chem. Soc. Rev. 37 (2008) 1568–1578.
- [6] J.B. Goodenough, Y.H. Huang, J. Power Sources 173 (2007) 1–10.
- [7] M.D. Gross, K.M. Carver, M.A. Deighan, A. Schenkel, B.M. Smith, A.Z. Yee, J. Electrochem. Soc. 156 (2009) B540–B545.
- [8] B.H. Smith, M.D. Gross, Electrochem. Solid-State Lett. 14 (2011) B1–B5.
- [9] J.H. Edwards, A.M. Maitra, Fuel Process. Technol. 42 (1995) 269–289.
- [10] S. Wang, G.Q. Lu, G.J. Millar, Energy Fuels 10 (1996) 896–904.
- [11] H.F. Abbas, W.M.A. Wan Daud, Int. J. Hydrogen Energy 35 (2010) 1160–1190.
- [12] J. Liu, B.D. Madsen, Z. Ji, S.A. Barnett, Electrochem. Solid-state Lett. 5 (2002) A122–A124.
- [13] X.B. Zhu, Z. Lü, B. Wei, K.F. Chen, M.L. Liu, X.Q. Huang, W.H. Su, J. Power Sources 190 (2009) 326–330.
- [14] G.L. Xiao, F.L. Chen, Electrochem. Commun. 13 (2011) 57–59.
- [15] Q.L. Ma, F. Tietza, A. Leonide, E. Ivers-Tiffée, Electrochem. Commun. 12 (2010) 1326–1328.
- [16] K.Q. Huang, R.S. Tichy, J.B. Goodenough, J. Am. Ceram. Soc. 81 (1998) 2565–2575.
- [17] Q. Liu, X.H. Dong, G.L. Xiao, F. Zhao, F.L. Chen, Adv. Mater. 22 (2010) 5478–5482.
- [18] G.L. Xiao, Q. Liu, X.H. Dong, K. Huang, F.L. Chen, J. Power Sources 195 (2010) 8071–8074.
- [19] K.H. Ryu, S.M. Haile, Solid State Ionics 125 (1999) 355–367.
- [20] X.B. Zhu, Z. Lu, B. Wei, X.Q. Huang, Y.H. Zhang, W.H. Su, J. Power Sources 196 (2011) 729–733.